Cao, Yan; Li, Yiqing; Zhang, Geng; Kittisak Jermsittiparsert; Nasseri, Maryam

Article

An efficient terminal voltage control for PEMFC based on an improved version of whale optimization algorithm

Energy Reports

Provided in Cooperation with:
Elsevier

Suggested Citation: Cao, Yan; Li, Yiqing; Zhang, Geng; Kittisak Jermsittiparsert; Nasseri, Maryam (2020) : An efficient terminal voltage control for PEMFC based on an improved version of whale optimization algorithm, Energy Reports, ISSN 2352-4847, Elsevier, Amsterdam, Vol. 6, pp. 530-542, https://doi.org/10.1016/j.egyr.2020.02.035

Energy Reports 6 (2020) 530–542

Contents lists available at ScienceDirect

Energy Reports

journal homepage: www.elsevier.com/locate/egyr

Research paper

An efficient terminal voltage control for PEMFC based on an improved version of whale optimization algorithm

Yan Cao [a], Yiqing Li [a], Geng Zhang [a], Kittisak Jermsittiparsert [b,*], Maryam Nasseri [c]

[a] School of Mechatronic Engineering, Xi'an Technological University, Xi'an, 710021, China
[b] Social Research Institute, Chulalongkorn University, Bangkok 10330, Thailand
[c] Department of Engineering, Ardabil Branch, Islamic Azad University, Ardabil, Iran

ARTICLE INFO

Article history:
Received 3 December 2019
Received in revised form 26 February 2020
Accepted 28 February 2020
Available online xxxx

Keywords:
Proton exchange membrane fuel cell
Parameter estimation
LQR
Whale optimization algorithm
Chaotic

ABSTRACT

Recently, the application of the proton exchange membrane fuel cells (PEMFCs) is extensively increasing as a popular renewable energy source. PEMFCs need low temperature for the operation along with high power density and easy implementation ability. These characteristics turned them into the most interesting type of fuel cells. However, PEMFCs need a technique for keeping them in a desired operating point. This is an essential item, especially during the current variation. In this study, a new configuration is proposed for designing an optimal PEMFC system. Two-phase interleaved boost DC/DC converter is also utilized for increasing the output voltage terminal. LQR optimal strategy is used for regulating the PEMFC. For improving the efficiency of the proposed LQR controller, a newly developed version of the whale optimization algorithm, called improved chaotic whale optimization algorithm is proposed. Simulation results of the proposed system are compared with different methods and the results showed that the proposed system has higher efficiency from the viewpoint of the current ripple and overshoot.

1. Introduction

Experts consider energy as the driving force for comprehensive economic development worldwide. The use of available energy sources is a major factor in the economic development of the post-human societies. Concerns about environmental changes along with the rising of the fossil fuel cost have created rules that encourage the commercialization and exploitation of highly renewable resources. Renewable energies are referred to as energy sources that unlike non-renewable energies, are capable of re-usability in nature (Alizadeh et al., 2016; Ebrahimian et al., 2018).

Solar, wind, geothermal, biomass, hydrogen, and fuel cells are some examples of renewable energy resources. The expiration of fossil fuel and nuclear fuel resources and also environmental degradation by pollutants from exploiting these energy sources has made renewable energies as an essential part of modern life. Fuel cells are one of the green renewable energy sources that have no pollutions by themselves (Jabbari et al., 2019; Yan et al., 2019). Moreover, their efficiency can be significantly higher than that of internal combustion engines.

The fuel cell is a conversion system for converting chemical energy into electricity. A fuel cell turns hydrogen and oxygen into the water to generate electricity during the process. The chemicals are continuously flowing inside the fuel cell, so the fuel cell does not end up as long as the fluid flows to the cell, and the electricity flows out. Hydrogen and oxygen include the main raw materials of the fuel cells (Yan et al., 2019; Lü et al., 2018). The fuel cell provides a DC (direct current) voltage that is usable and sufficient to supply motors, lights, or any number of electric vehicles (Liu et al., 2017; Aghajani and Ghadimi, 2018). In recent years, the application of fuel cell technology is continuously increasing for portable and stationary usages. Some advantages of the fuel cells are given below:

- By controlling the number of reactive substances (hydrogen and oxygen), the power output of the fuel cell can be controlled.
- Because hydrogen is used as the primary fuel, its output is only water, and there is not any noise pollution due to the absence of mechanical parts.
- Hydrogen can be supplied from different sources such as water, natural gas, coal, methanol, and hydrocarbon fuels.
- Fuel cells have the highest energy storage densities compared with batteries, electrochemical capacitors, and super-capacitors.

Several works have been performed on developing the electrolyte type fuel cells (Mekhilef et al., 2012; Ahmadi and Kjeang,

* Corresponding author.
E-mail address: kittisak.j@chula.ac.th (K. Jermsittiparsert).

https://doi.org/10.1016/j.egyr.2020.02.035

2015). Among different types of these fuel cells, polymer electrolyte membrane (PEM) has some prominent characteristics that make the researchers work more on them.

The available operating range for the voltage of the polymer electrolyte membrane in the market is between 26 V and 50 V. The application of PEM fuel cells is increasing in different places from portable devices, industrial systems, and places where there is a need for stationary and residential power (Khodaei et al., 2018). Although PEM fuel cells have an efficiency between 40% and 60% during electricity production, their efficiency can be increased by up to 85% by using them as combined heat and power (CHP) systems (Jin et al., 2006). Due to the PEM fuel cells' thermodynamic and electrochemical nature, they are not suitable to utilize for loads that have sudden changes. Therefore, utilizing a power conditioning step for regulating the source signal of the load demands and for achieving the maximum power is an essential term (Mwinga et al., 2018; Mayo-Maldonado et al., 2019).

Another problem is that because of the limitation of the generated voltage in the fuel cells around 1 V, it needs a technique for increasing the voltage level as far as it can be used for practical applications. A simple method is to use a serial configuration of the fuel cells which is not very efficient due to some mechanical limitations. Another way is to utilize DC/DC converters (Sanghavi et al., 2019). Since the DC/DC converter is a significant part of the PEM power conditioning unit, in this study the integration of the converter besides the PEM fuel cell is considered. Generally, designing a proper converter has a vital influence on power regulation, especially on common DC buses. Several research works have been performed about using the DC–DC converters in the fuel cells (Sabzali et al., 2015; Al-Saffar and Ismail, 2015; Zhang et al., 2017).

Among different converters, boost converter can result in a system with higher performance and a lower number of elements for interfacing the fuel cell and the load (Huangfu et al., 2017). Multi-level converters can meet this goal. The interleaved boost DC/DC converter (IBC) is a component that can resolve this issue (Gules et al., 2003; Hegazy et al., 2012; Dwari and Parsa, 2011). PEM fuel cells generate a high current that forces them to utilize oversized coils. One problem is that high ripple in current is not idealistic and decreases the operational lifetime of the PEM fuel cell membrane. The proper selection of duty cycle level and the phase number make the current ripples to be approximately zero. Other advantages of the IBC include power level improvement, current stress minimization, and inductor size reduction (Giral et al., 2000).

In 2018, Ma et al. proposed a method based on robust control for regulating the DC/DC boost converter in the PEM fuel cells. The main idea was based on using a high-order super-twisting sliding mode control to achieve this purpose. For analyzing the impact of the presented method, it was verified on a buck/boost converter under different operating conditions. Experimental results showed that the proposed method gives a robust and feasible solution for real-time applications (Ma et al., 2018).

In 2018, Reddy et al. presented an IBC converter along with RBF neural network to obtain the maximum power point tracking in a fuel cell for electric vehicle application through a high voltage-gain boost converter (Reddy and Sudhakar, 2018). To obtain a high voltage-gain, the IBC converter was also designed. The method decreased the input current ripple and voltage stress on the power semiconductor components. Buswig et al. also proposed similar work in Buswig et al. (2018).

In 2017, Ahmadi et al. proposed an optimal PID controller for the maximum power point tracking of a PEM fuel cell based on particle swarm optimization (PSO) algorithm. The main structure of the system was a PEM fuel cell, a boost converter, a battery, and a PSO–PID controller. The controller was utilized for tuning the operating point of the PEM fuel cell based on adjusting the duty cycle. The final results were compared with *perturb and observe* (P&O) and sliding mode (SM) algorithms under various operating conditions which showed the method's high precision, fast convergence, and its very low power fluctuations in tracking the maximum power point of the system (Ahmadi et al., 2017). Some related works can be found in Banerjee et al. (2017), Razmjooy et al. (2016a), Khalilpour et al. (2013) and Razmjooy and Khalilpour (2015). In 2018, Abdul Basit et al. presented a method for the voltage tracking of a DC/DC Boost Converter including fuel cell based on the neuro-fuzzy method (Basit and Badar, 2018).

In this study, different types of Neuro-Fuzzy systems were compared and studied for the emergency landing scenario of More Electric Air-Craft. Simulation results were compared among the traditional Neuro-Fuzzy, ANFIS wavelet control, Takagi Sugeno Kang (TSK) control, and classical PI control. More works about neuro-fuzzy can be found in Hameed et al. (2018), Mousavi et al. (2013) and Razmjooy et al. (2017). There are also some more works that can be studied in Kolli et al. (2015), Wang et al. (2019) and Guida et al. (2019). Since the nature of both IBC converter and PEM fuel cell is highly nonlinear, using linear controllers in their structure is not a good idea. For removing the voltage and the current ripples, IBC has been used (duty-cycle for two-phase IBC is 0.5). For simplifying the control process, the IBC model is first linearized around the duty cycle and then, it is controlled by a linear controller.

Because of the low-level voltage generation in the polymer electrolyte membrane fuel cell systems, a proper method is required for controlling the voltage terminal.

Linear Quadratic Regulator (LQR) is another simple and easy to implement method for the optimal control of PEMFCs. This method has different advantages such as an optimal solution. But there is also one big drawback to this technique. The parameters "R" and "Q" are achieved based on trials and errors. This reason makes it sensitive to the changes. In this study, a new feedback control configuration is designed based on the linear quadratic regulator (LQR) algorithm and the IBC. Since the LQR parameter selections are based on trials and errors, an optimization algorithm is introduced here to the optimal selection of these parameters. An optimized feedback controller is designed using the LQR technique and a new optimization algorithm called improved chaotic whale optimization algorithm.

The new algorithm is an improved version of the whale optimization algorithm based on chaos theory. Final results showed that using the introduced whale optimization algorithm has higher efficiency than the original whale optimization algorithm and some other state of the art methods.

The novelty and contributions of the proposed paper are summarized as follow:

- A new method for achieving the optimal output from Proton Exchange Membrane Fuel Cell has been introduced.
- A new optimized LQR system is proposed.
- An improved WOA based on Chaos theory is proposed to improve its performance.
- Sinusoidal chaotic maps have been utilized to adjust the key parameter 'p' of WOA.
- The proposed CWOA is validated on the interleaved boost DC/DC converter
- Statistical results applied to the control system of the Proton Exchange Membrane Fuel Cell and the results are compared by popular works

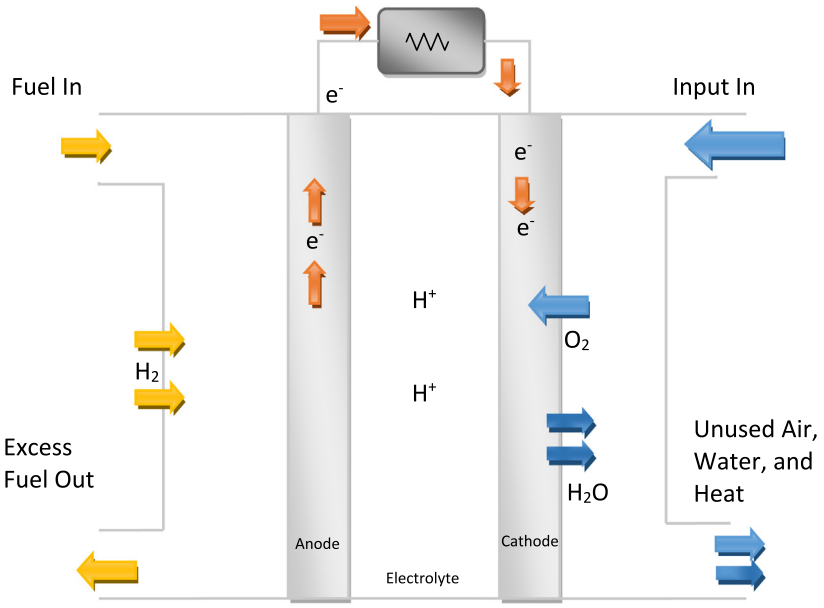

Fig. 1. The general model of a fuel cell.

The organizations of the sections are explained in the following. Sections 2 and 3 describe the general mathematical model of the proton exchange membrane and the interleaved boost converter. In Section 4, a general statement of the problem is proposed. Section 5 presents the proposed newly developed optimization algorithm, whale optimization algorithm. In Section 6, the proposed optimal LQR Control System based on the improved Chaotic Whale Optimization Algorithm has been proposed. Section 7 illustrates the results of the simulation and the comparison of the system by other methods and the paper is concluded in Section 8.

2. Mathematical model of proton exchange membrane

In this section, the mathematical modeling of the Proton Exchange Membrane fuel cell (PEMFC) is presented. The basic function of PEMFCs is to use of hydrogen and oxygen in the air to generate electricity. In a PEMFC, the membrane is an electrolyte that is used to separate the two half-cell reactions, block electrons and allow for protons transferring. The catalytic environment is provided by the platinum electrocatalyst on both sides.

Anode allows Hydrogen gas to pass through with the help of a catalyst to split the gas into electrons and hydrogen protons. Hydrogen gas passes over one electrode called an anode and then with the help of a catalyst, splits it into electrons and hydrogen protons. Fig. 1 shows this process.

The process of chemical reaction in the PEMFC can be described as follows (Jalili and Ghadimi, 2016):

$$2H_2 + O_2 \rightarrow 2H_2O + heat + electricity \tag{1}$$

It can also be described as follow:

$$H_2 \rightarrow 2H^+ + 2e^- \tag{2}$$

$$\frac{1}{2}O_2 + 2H^+ + 2e^- \rightarrow H_2O \tag{3}$$

$$H_2 + \frac{1}{2}O_2 \rightarrow H_2O \tag{4}$$

where, H_2, O_2, and H_2O are hydrogen (as fuel), oxygen (as Oxidant), and water, respectively.

The terminal voltage of the fuel cell can be achieved by the following equation (Jalili and Ghadimi, 2016):

$$V_{FC} = E_{OC} - (V_{AL} + V_{OL} + V_{CL}) \tag{5}$$

where, E_{OC} presents the open-circuit voltage, and V_{AL}, V_{OL}, and V_{CL} are activation, Ohmic, and concentration losses, respectively.

2.1. Open circuit voltage model of the PEMFC

By considering the Nernst equation, the open-circuit voltage model for the PEMFC is defined as follows (Lee et al., 2006):

$$E_{OC} = 1.30 - 0.85e^{-3} \times (T_{CT} - 298.15) + 4.31e^{-5}T_{CT} \times [\ln(P_{H_2}) + 0.5\ln(P_{O_2})] \tag{6}$$

where, T_{CT} describes the cell's temperature (Kelvin) and P_{O_2} and P_{H_2} are the partial pressure of oxygen (bar) and hydrogen (bar), respectively.

2.2. Activation losses of the PEMFC

The activation loss for the PEMFC can be described by the following formula (Morsali et al., 2015):

$$V_{AL} = V_{L_{oc}} + V_a(1 - e^{-c_1^i}) \tag{7}$$

where, $V_{L_{oc}}$ is the voltage loss in the open circuit mode (V), and V_a and c_1 are constants that can be achieved experimentally.

2.3. Ohmic losses of the PEMFC

The Ohmic loss for the PEMFC is mathematically modeled by the following formula (Morsali et al., 2015):

$$V_{OL} = i \times \frac{t_m}{\sigma_m} \tag{8}$$

where, $\frac{t_m}{\sigma_m}$ defines the internal resistance (Ω cm^2), t_m describes the membrane thickness, and σ_m is the conductivity of the membrane. Note that the resistance, the internal temperature, and the humidity of the membrane dependent on each other.

2.4. Concentration losses of the PEMFC

The *Concentration* loss of the PEMFC can be presented by the following equation (Morsali et al., 2015):

$$V_{CL} = i \times \left(c_2 \times \frac{i}{I_{\max}}\right)^{c_3} \tag{9}$$

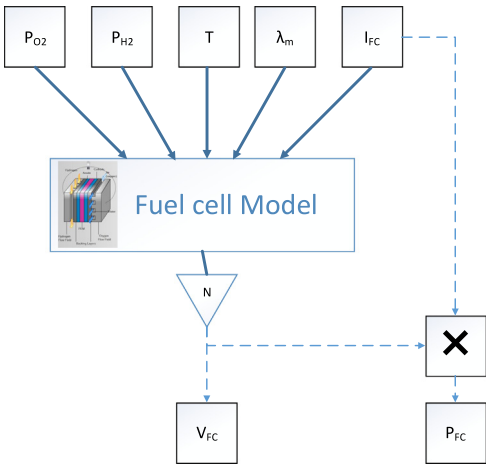

Fig. 2. The PEMFC voltage simulink model.

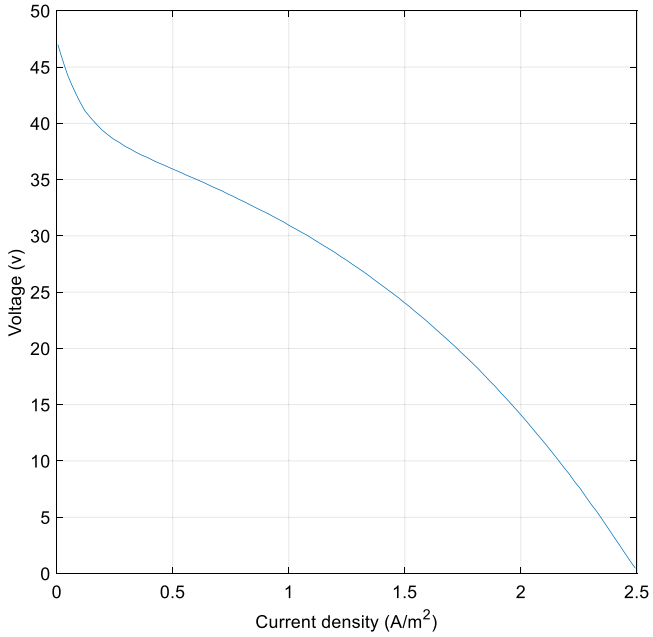

Fig. 3. PEMFC voltage — current density characteristic.

where, $I_{\max}$ describes the density of the current which generates abrupt voltage drop. c_2, c_3, and $I_{\max}$ depends on the reactant partial pressure and the temperature and are achieved experimentally.

Finally, the terminal current and voltage of the fuel cell stack can be achieved as follows:

$$I = \frac{I_{FC}}{A_{FC}} \tag{10}$$

$$V_T = N \times V_{CL} \tag{11}$$

where, N is the number of cells and A_{FC} is the active surface of the cells, and I is the current density.

The Simulink model for the voltage of a PEMFC is shown in Fig. 2.

The voltage–current and the power–current diagrams for the Proton Exchange Membrane fuel cell are given in Figs. 3 and 4, respectively.

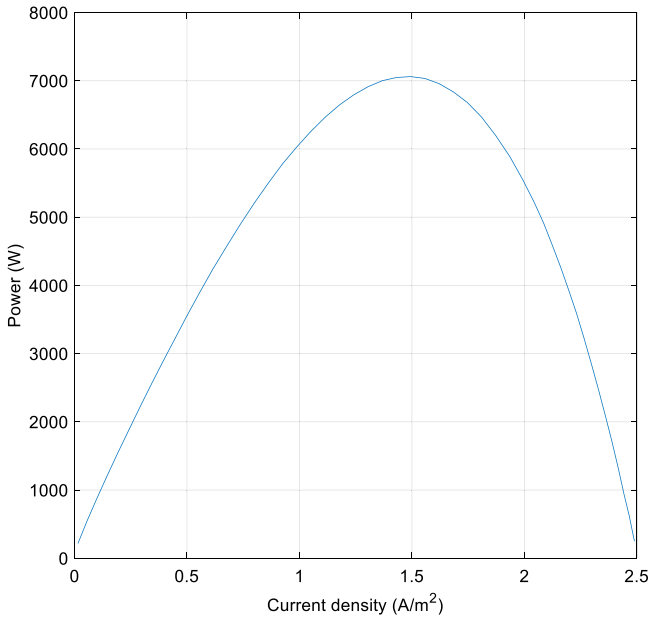

Fig. 4. PEMFC power — current density characteristic.

3. Mathematical model of the interleaved boost converter

In this study, the two-phase interleaved boost converter (IBC) is utilized for the aforementioned regulation system. A simple way to generate an interleaved boost converter is to connect the inputs and the outputs of two boost converters while considering the shifting drive signals in 180° (Guilbert et al., 2015; Ghadimi and Firouz, 2015; Habib et al., 2017).

The two-phase IBC has two operating modes. The first mode contains the conditions that the duty cycle is lower than the 50% and the second mode is for the operation mode when the duty cycle is higher than the 50%. In the event that the duty cycle is exactly 50%, there will be a complete ripple cancellation. Therefore, in this condition, the ripple in the input and the output signals are zero and minimum, respectively.

The original model of the IBC has interval uncertainties. So, to control this system in a practical condition, the mean value of the uncertainties is selected for the system control. The mean value of the IBC is somehow similar to the ordinary boost converter, of course with two current inductances.

$$\begin{aligned} L_1\frac{dI_{L1}}{dt} &= V_T - V_{ca}(1-D_1)\\ L_2\frac{dI_{L2}}{dt} &= V_T - V_{ca}(1-D_2)\\ I_{FC} &= I_{L1} + I_{L2}\\ C\frac{dV_{ca}}{dt} &= I_{L1}(1-D_1) + I_{L2}(1-D_2) - I_{ch} \end{aligned} \tag{12}$$

where, V_T and V_{ca} describe the total voltage and the capacitor voltage, respectively, $D_1 = D_2 = D$ describe the duty cycle of the phases, $L_1 = L_2 = L$ represents the phases inductance, and C is the phases capacitor.

Fig. 5 shows the general architecture of the interleaved boost converter with two phases and Fig. 6 shows the current and source current Inductances. In Fig. 6, x-axis and y-axis show the duty cycle and the current amplitude, respectively.

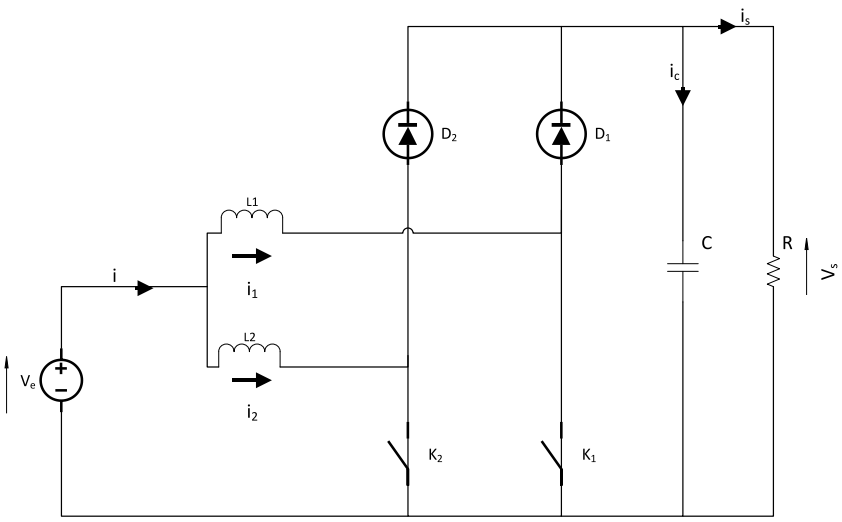

Fig. 5. The general architecture of the interleaved boost converter.

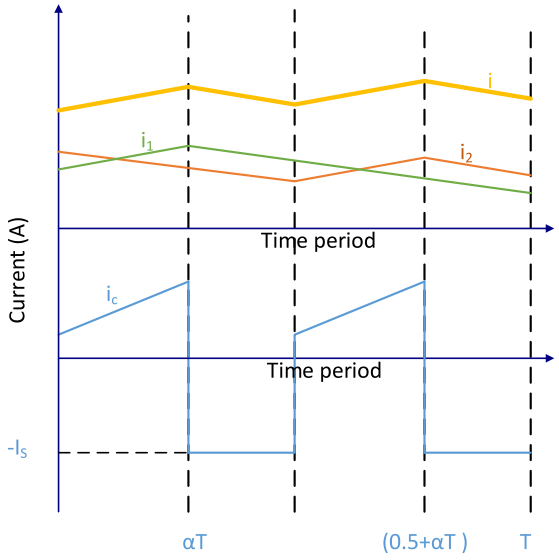

Fig. 6. The current and the source current inductances for $\alpha < 0, 5$.

The state-space model of the IBC system is defined as follows:

$$A_{state} = \begin{bmatrix} 0 & 0 & x \\ 0 & 0 & x \\ y & y & -\dfrac{1}{RC} \end{bmatrix}, \; state \begin{cases} if \;\; ON: x = -\dfrac{1}{L}, \;\; y = \dfrac{1}{C} \\ if \;\; OFF: x = y = 0 \end{cases}$$
$$B_{ON} = B_{OFF} = \begin{bmatrix} -\dfrac{1}{L} & 0 & 0 \\ 0 & -\dfrac{1}{L} & 0 \end{bmatrix}^T \tag{13}$$

where, the state and the control vectors are presented below.

$$X = \begin{bmatrix} I_L & I_L & V_C \end{bmatrix}^T$$
$$U = \begin{bmatrix} D & D \end{bmatrix}^T \tag{14}$$

By linearizing the model around the equilibrium points:

$$X_0 = \begin{bmatrix} V_T/RD_d'^2 & V_T/RD_d'^2 & V_T/D_d' \end{bmatrix}^T$$
$$U_0 = [D_d \quad D_d]^T \tag{15}$$

where, $D_d' = 1 - D_d$ describes the duty cycle of the complementary operating points.

Afterward, an augmented state variable (x_3) is added to the model that is considered as:

$$x_3 = -\int V_c \tag{16}$$

where, the state error is zero.

Based on the considered equilibrium point and withdrawing the nonlinear part of the system model, the linearized additional model can be described as follows:

$$\begin{cases} x = X_0 - X, \\ u = U_0 - U \end{cases}$$
$$\dot{x} = Ax + Bu \tag{17}$$

Therefore, the final state-space model of the system is obtained as follows:

$$A = \begin{bmatrix} 0 & 0 & -\dfrac{D_d'}{L} & 0 \\ 0 & 0 & -\dfrac{D_d'}{L} & 0 \\ \dfrac{D_d'}{C} & \dfrac{D_d'}{C} & -\dfrac{1}{RC} & 0 \\ 0 & 0 & -1 & 0 \end{bmatrix}, \; B = \begin{bmatrix} \dfrac{V_T}{D_d'L} & 0 \\ 0 & \dfrac{V_T}{D_d'L} \\ -\dfrac{V_T}{RCD_d'^2} & -\dfrac{V_T}{RCD_d'^2} \\ 0 & 0 \end{bmatrix} \tag{18}$$

4. Problem statement LQR definition

Consider an LTI system as follows:

$$\dot{X}(t) = AX(t) + BU(t),$$
$$Y(t) = CX(t) + DU(t) \tag{19}$$

where, $A \in \mathrm{R}^{m \times m}$, $B \in \mathrm{R}^{m \times n}$, $C \in \mathrm{R}^{q \times m}$, $D \in \mathrm{R}^{q \times n}$.

The main purpose in the LQR optimal control is to minimize the following performance index (Razmjooy et al., 2016b, 2014):

$$J(U^*) = \int_0^\infty \left(X^T(t) Q X(t) + U(t)^T R U(t) \right) dt \tag{20}$$

where, Q and R are positive semi-definite and positive definite, respectively.

Generally, in LQR, the weighting matrices, Q and R have a significant effect on the final performance results. The size of R

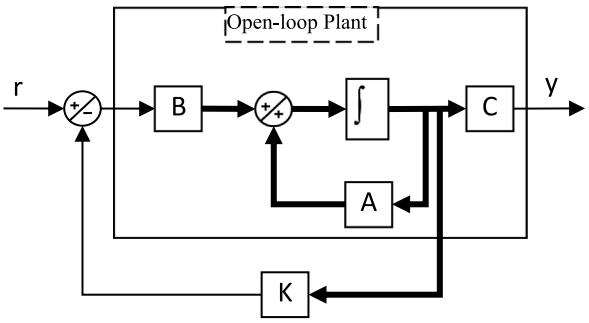

Fig. 7. The main structure of the LQR controller.

and Q directly depend on the number of the input and the state variables, respectively. Fig. 7 shows the general configuration of the LQR controller.

5. Improved chaotic whale optimization algorithm

Optimization is the process of finding the best acceptable solution for a problem by considering the system dynamic and its constraints. The meta-heuristic algorithm is a kind of optimization algorithms that is inspired by nature, physics, and human social reactions and is used to solve different types of optimization problems. In most cases, these algorithms are used in combination with other algorithms to reach the advantages of all combined algorithms to escape from the local optimum.

Some of these algorithms are like Genetic algorithm (Ebrahimian et al., 2018; Khodaei et al., 2018; Holland, 1992; Mirjalili, 2019; Mousavi and Soleymani, 2014), particle swarm optimization (Moallem and Razmjooy, 2012; Razmjooy and Ramezani, 0000), quantum invasive weed optimization (Razmjooy and Ramezani, 2014), Cooperative bat searching algorithm (Hamian et al., 2018), Parallel Multiagent Coordination Optimization Algorithm (Zhang and Hui, 2016; Gollou and Ghadimi, 2017), and world cup optimization algorithm (Razmjooy et al., 2016a) which have been designed for solving different complicated optimization problems. In recent years, Razmjooy et al. presented the basic version of the world cup optimization algorithm (WCO) and employed on different problems (Razmjooy et al., 2016a; Bandaghiri et al., 2016; Razmjooy et al., 0000; Razmjooy and Shahrezaee, 0000; Razmjooy et al., 2018; Shahrezaee, 2017) which inspired by the FIFA world cup competitions to reach up to the championship as an optimal solution.

5.1. Classic whale optimization algorithm

In Mirjalili and Lewis (2016), Mirjalili and Lewis presented the basic version of the whale optimization algorithm (WOA) and employed it on different problems (Mafarja and Mirjalili, 2017; Oliva et al., 2017; Mirzapour et al., 2019). The algorithm is inspired by the whale's ability for hunting prey as an optimal solution. The hunting process of the whale is mathematically modeled as an optimization problem to find the global optimum (maximum or minimum). The main purpose in WOA is to search for prey and hunting them by two procedures, including encircling the prey and then generating bubble nets around them to surround them. Like most of the other optimization algorithms, WOA has two parts of exploration (seeking for the prey) and exploitation (hunting strategy) (Mirjalili and Lewis, 2016). WOA starts with a random vector of the solution including the population to seek and to find the global optimum (maximum or minimum) solution of the problem. Afterward, the algorithm uses the two above aforesaid strategies to update and to find the best solution. The bubble-net system in the humpback whales can be mathematically modeled as the following equation:

$$X(t+1) = \begin{cases} X^*(t) - AD & p < 0.5 \\ D' e^{bl} \cos(2\pi t) + X^*(t) & p \geq 0.5 \end{cases} \tag{21}$$

$$D' = \left| CX^*(t) - X(t) \right| \tag{22}$$

$$A = 2ar - a \tag{23}$$

$$C = 2r \tag{24}$$

where, l is a random constant in the interval $[-1, 1]$, r and p are random constants in the range [0,1], a *is* descent from 2 to 0 linearly over the iteration. t describes the current iteration, b defines the logarithmic shape of the spiral motion, D' illustrates the distance for ith whale from the best solution (pray).

It is better to know that for guaranteeing the convergence of the algorithm, the best solution improves the position of the agents when $|X| > 1$.

It is important to know that using random whales instead of best whale can improve the model as follows:

$$D' = |CX_{rand}(t) - X(t)| \tag{25}$$

$$X(t+1) = \begin{cases} X_{rand}(t) - AD & p < 0.5 \\ D' e^{bl} \cos(2\pi t) + X_{rand}(t) & p \geq 0.5 \end{cases} \tag{26}$$

The results of the proposed WCO algorithm are good, but they have one drawback; the traditional WCO has rather a weakness from the point of convergence speed.

In this paper, a chaos function is utilized for increasing the convergence speed such that the iteration for the new populations is obtained based on the chaos theory (not completely random) to increase the algorithm speed (Leng et al., 2018; Schymura and Kolossa, 2019).

5.2. The conception of chaotic theory

The chaos theory is the study of seemingly random unpredictable behavior in a system controlled by definite rules. Some complicated nonlinear dynamical systems have chaotic nature such that they behave randomly and unpredictably. The main purpose of the chaos theory is to study nonlinear and highly sensitive systems relative to the initial conditions. In other words, a small difference in the initial condition, make high variations in the system behavior. The main characteristics of a chaotic system can be considered as follows: random behavior and sensitivity to the primary condition. Therefore, by considering this property, a high diversity for the population can be generated to improve the global optimum capability and to escape from trapping in a local optimum (Yang et al., 2007; Akbary et al., 2019).

A discrete-time dynamical definition for the chaos is presented below.

$$\begin{aligned} &CM_{i+1}^j = f(CM_i^j) \\ &j = 1, 2, \ldots, k \end{aligned} \tag{27}$$

where, k describes the map dimension, $f(CM_i^j)$ is the chaotic model generator function and can be described by different maps.

5.3. The improved chaotic whale optimization algorithm

In this subsection, an improved version of the WOA is proposed based on the sinusoidal chaotic map. The proposed method is called Improved Chaotic Whale Optimization Algorithm (ICWOA). The main profit of the proposed method from the classic WOA method is that it can escape from the local optimal following by high speed in convergence. In the proposed ICWOA,

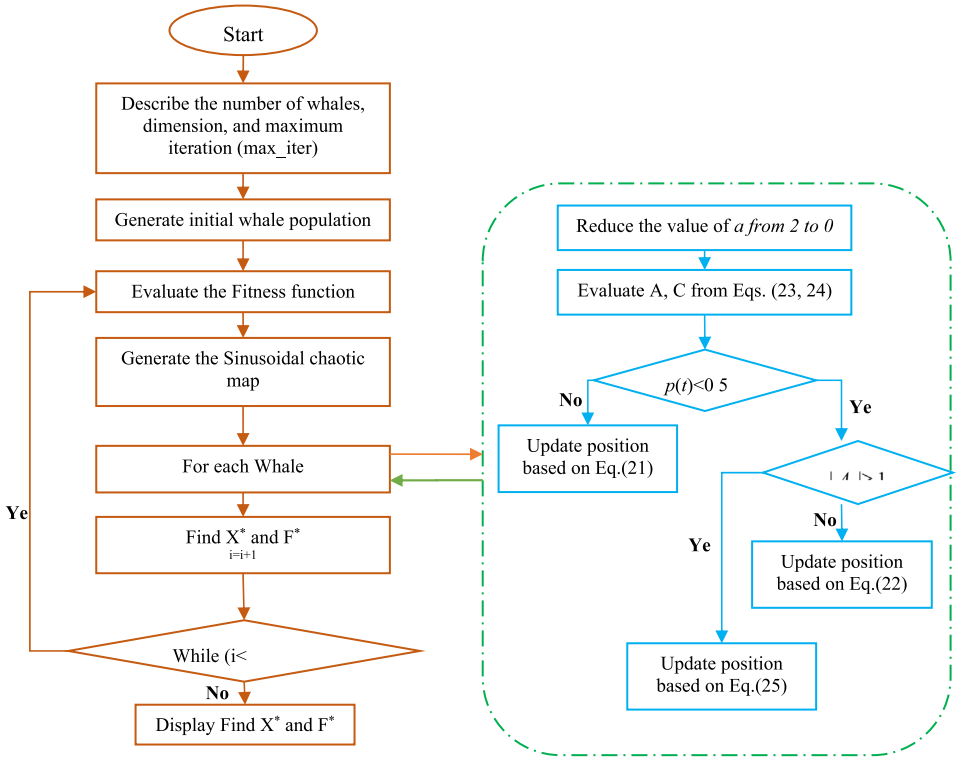

Fig. 8. The flowchart diagram of the proposed ICWOA.

Table 1
The utilized benchmarks for efficiency analysis.

Benchmark	Formula	Constraints	Dimension
Rastrigin	$f_1(x) = 10D + \sum_{i=1}^{D} \left(x_i^2 - 10\cos(2\pi x_i)\right)$	[−512, 512]	30–50
Rosenbrock	$f_2(x) = \sum_{i=1}^{D-1} \left(100\left(x_i^2 - x_{i+1}\right) + (x_i - 1)^2\right)$	[−2.045, 2.045]	30–50
Ackley	$f_3(x) = -20\exp\left(-0.2\sqrt{\frac{1}{D}\sum_{i=1}^{D} x_i^2}\right) - \exp\left(\frac{1}{D}\sum_{i=1}^{D}\cos(2\pi x_i)\right) + 20 + e$	[−10, 10]	30–50
Sphere	$f_4(x) = \sum_{i=1}^{D} x_i^2$	[−512, 512]	30–50

parameter probability (prob) value from Eq. (21) is modeled based on the sinusoidal chaotic map as follows.

$$p_{k+1} = a p_k^2 \sin(\pi p_k)$$
$$p_0 \in [0, 1],\ a \in (0, 4] \quad (28)$$
$$k \text{ is iteration number}$$

This improvement makes the spiral model selection easy for updating the location of the whales. Fig. 8 shows the flowchart diagram of the proposed ICWOA

The parameters of the controller should be justified as locations of the whales. The dimension of the search space presents the parameter numbers of the LQR controller.

5.4. Validation of the ICWOA

For efficiency analysis of the proposed ICWOA, four standard functions have been validated. The results of the proposed algorithm (ICWOA) are also compared with some different algorithms including genetic algorithm (GA) (Holland, 1992), particle swarm optimization algorithm (PSO) (Bansal, 2019), world cup optimization algorithm (WCO) (Razmjooy et al., 2016a), and standard whale optimization algorithm (WOA) (Mirjalili and Lewis, 2016).

The simulations are applied by Matlab R2017b with a PC configuration of 2.50 GHz CPU and 16.0 GB RAM. Table 1 illustrates the benchmarks formulations that are used for the performance analysis.

Table 2 illustrates the mead deviation (MD) and the standard deviation (SD) values for the analyzed benchmarks.

Form Table 2, it is obvious that using the proposed method provides the best result toward the other state of the art methods on f_1, f_2, and f_4 and the results on f_3 is better than GA, PSO, WCO, but the same as the original WOA.

6. Optimal LQR control system based on improved chaotic whale optimization algorithm

There are different improvements to the Whale Optimization Algorithm which can be found in Mafarja and Mirjalili (2017), Oliva et al. (2017) and Morsali et al. (2014). The main purpose of the proposed chaotic based whale optimization algorithm here is to improve the ability of the exploration and the convergence speed in the algorithm.

The main purpose here is to find the optimal value for the weighting matrices including Q and R in the LQR controller. For simplifying the performance index as a quadratic term, diagonal matrices have been selected for the weighting matrices (Murray, 2010; Kwakernaak and Sivan, 1972; Nazarathy and Pulemotov, 2012; Hespanha, 2005; Ajasa and Sebiotimo, 0000). The performance index for the LQR system is described as $J(U^*)$ in Eq. (20). The matrix of the unknown weighting of the LQR including Q and

Table 2
The results of the efficiency analysis by considering 30-dimensions.

Benchmark		Proposed ICWOA	GA (Holland, 1992)	PSO (Bansal, 2019)	WCO (Razmjooy et al., 2016a)	WOA (Mirjalili and Lewis, 2016)
f_1	MD	0.00	70.61	74.24	2.19	2.58
	SD	0.00	1.66	8.96	4.35	2.14
f_2	MD	8.41	35.41	200.1	13.16	8.47
	SD	1.39	27.15	59.00	4.62	1.73
f_3	MD	3.17e−16	3.19e−2	8.26	3.14e−3	3.17e−16
	SD	0.00	2.14e−2	1.19	1.12e−3	0.00
f_4	MD	0.00	1.15e−4	8.27e−4	6.19e−9	9.65e−11
	SD	0.00	3.14e−5	5.12e−4	3.28e−9	9.83e−17

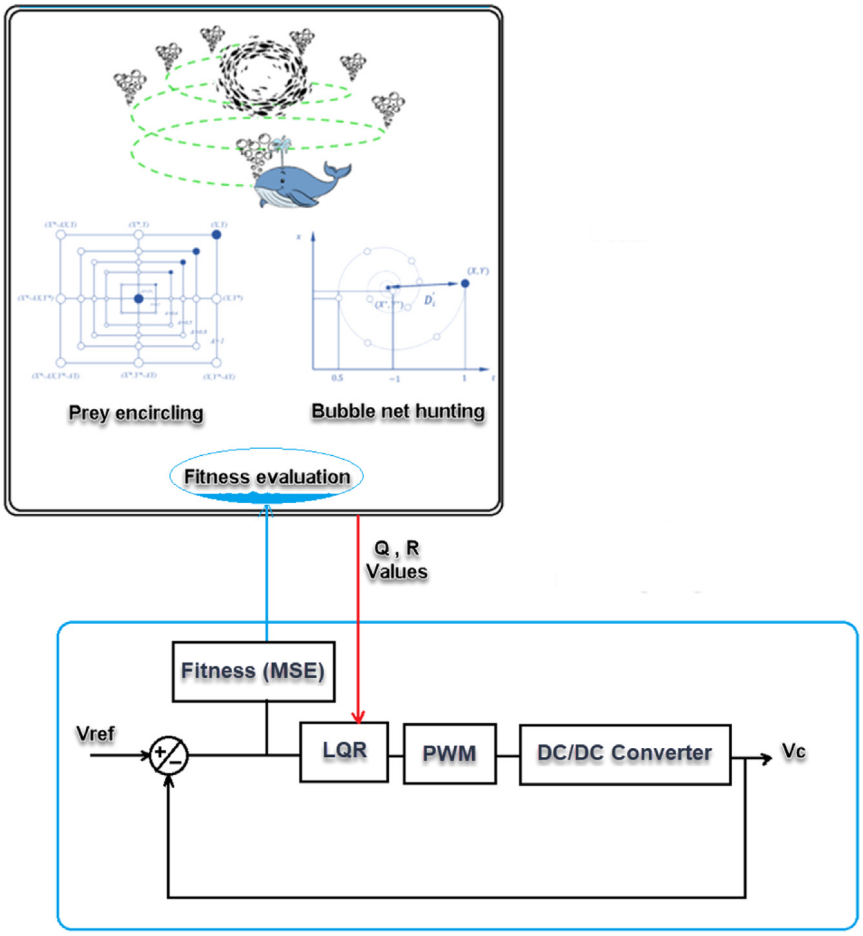

Fig. 9. The architecture of the proposed controller method.

R is given below:

$$Q = \begin{bmatrix} q_1 & 0 & 0 & 0 \\ 0 & q_2 & 0 & 0 \\ 0 & 0 & q_3 & 0 \\ 0 & 0 & 0 & q_4 \end{bmatrix}, \quad R = \begin{bmatrix} r_1 & 0 \\ 0 & r_2 \end{bmatrix} \tag{29}$$

In this study, the proposed method is utilized to solve the LQR optimization problem for the voltage control of the PEMFC.

The reason for using an optimization algorithm to solve the Riccati equation in LQR is to the optimal selection of the parameters Q and R; because, in the normal LQR, these parameters have been selected based on trial and error which makes the normal LQR to have an inaccurate optimal solution. By initializing the population for humpback whales, the proposed ICWOA evaluates the corresponding global best of the whale population that is achieved after the fitness function minimization. The cost function can be considered for the convergence of the optimization algorithms against the global optimal solution. In this study, the integral of the time-weighted absolute error (ITAE) is utilized as the cost functions of the state feedback controller structure.

$$ITAE = \int_0^T t\ |e(t)|\ dt \tag{30}$$

As before said, the purpose of the optimization here is to search for a feedback controller matrix such that the cost function of the ICWOA is minimized following by proper selection of the LQR parameters.

Fig. 9 shows the proposed control strategy for the PEMFC system which includes an LQR controller in association with ICWOA for optimal control of the PEMFC system.

7. Simulation results

As presented before, the main purpose of this paper is to optimal control of the interleaved boost regulator in the proton exchange membrane fuel cell based on the LQR control strategy.

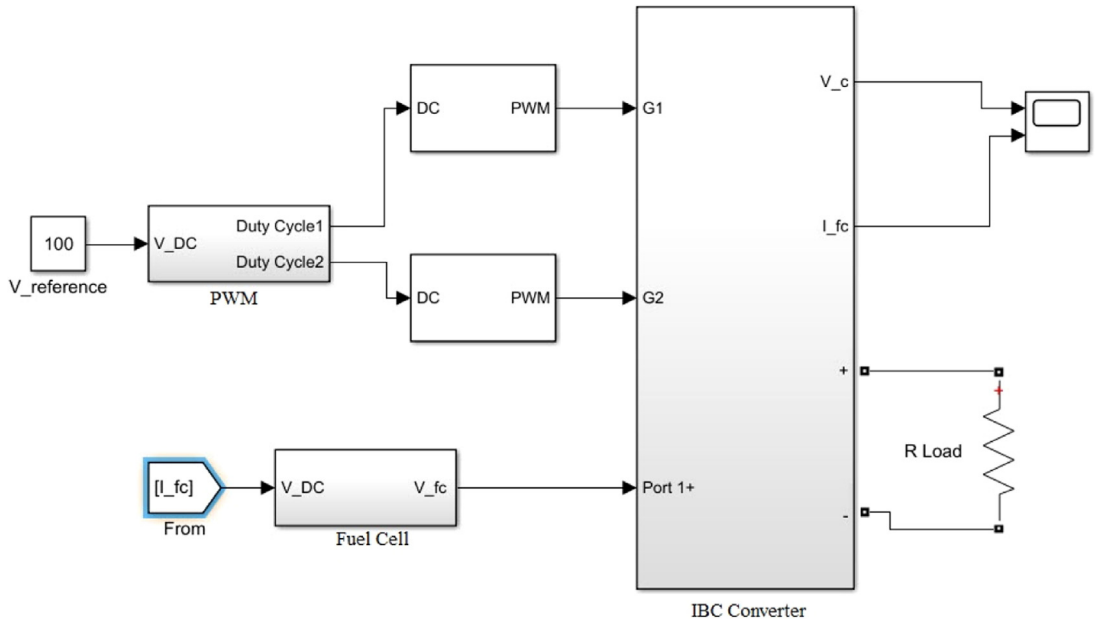

Fig. 10. General schematic of the proposed optimized PEMFC.

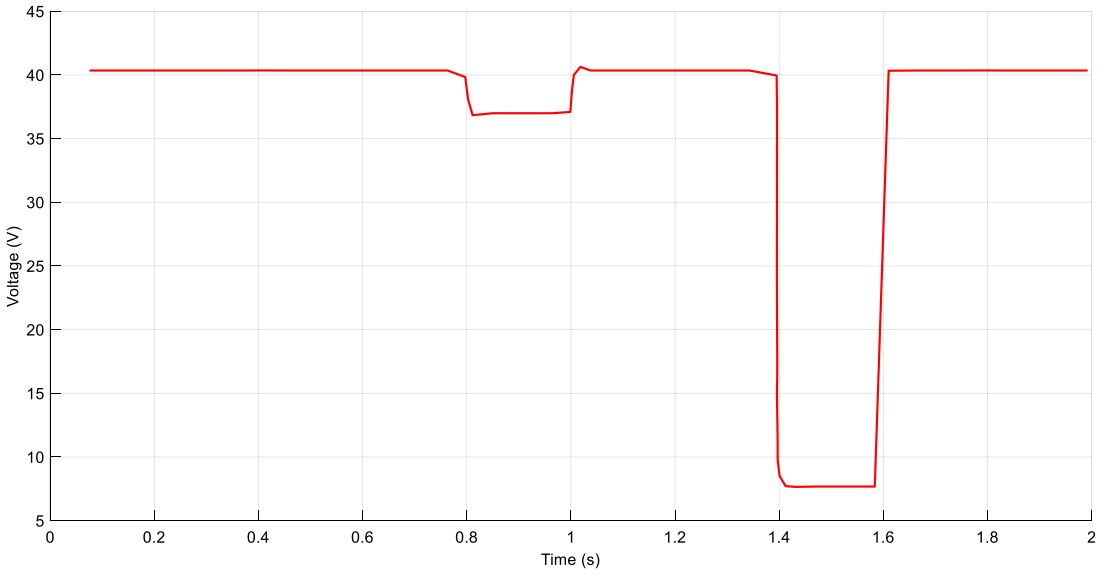

Fig. 11. The system analysis by the current load variation.

One of the most important problems of the LQR controller is to determine the weighting matrices, Q and R. These matrices are usually achieved after a lot of attempts while they are not guaranteed to be included in the best condition after all. The main idea of this study is to study proton exchange membrane fuel cell with two-phase interleaved boost DC/DC converter regulated by a new optimized method of the LQR based on the improved chaotic whale optimization algorithm. Because the interleaved boost converter is based on PWM switching, for avoiding the simultaneous switching, it is required to shift the modular number one by half of the period compared with the modular number two.

For validating the proposed optimized controller, the simulation model is performed by MATLAB/Simulink environment on the Intel® Core™ i7-4720 HQ CPU@2.60 GHz with 16 GB RAM. For the proposed ICWOA, the Number of Search Agents and the maximum iteration is selected 30 and 500, respectively. MATLAB Simulink Model of the simulation is shown in Fig. 10.

In the following, the results of the applying of the proposed ICWOA on the LQR controller have been explained based on minimizing the objective function. The main purpose of this research is to find an optimal feedback gain to evaluate the control signal U based on the parameters Q and R obtained with ICWOA to make the PEMFC stable.

The input matrix (B) is contained in the duty cycle evaluation and depends on the load current (I_L) and the voltage of the fuel cell (V_{FC}) as follows:

$$I_L = \frac{V_{FC}}{RD'_d} = \frac{V_s}{R} \tag{31}$$

where, I_L is the load current and V_s describes the desired voltage at the output for the interleaved boost DC/DC converter.

For performance analysis of the proposed system, it is compared with the traditional LQR (Habib and Khoucha, 2015), GA based LQR (Habib et al., 2017), traditional PI controller (Wang and

Table 3
System parameters (Habib and Khoucha, 2015).

Parameters of the proton exchange membrane fuel cell		
Parameter	Symbol	Value
Nominal voltage	V_n	47 V
Value of the voltage in 1 A	V_1	44 V
Open circuit voltage of the fuel cell	E_{oc}	1.22 V
Nominal current	I_n	30 A
The resistance of the membrane	R_m	0.079 Ω
Maximum power	P_{Max}	7 kW
The pressure of the hydrogen partial H_2	P_{O2}	0.3 bar
Temperature	T	80 °C
Constant	N	50
Sensor	λ_m	14
The pressure of the hydrogen partial O_2	P_{H2}	2.61 bar
Surface	A	200 cm^2
Parameters of the interleaved boost converter		
Parameter	Symbol	Value
Resistance	R	50 Ω
Inductance	$L_1 = L_2 = L$	0.005 H
Capacitor	C	0.001 F
The voltage of fuel cell at nominal current	V_g	46 V
Frequency of the switching	f	10 kHz
Desired voltage	V_s	100 V

Ko, 2010), and the original WOA based LQR (Qazi et al., 2018) to show its efficiency.

By considering the stability analysis, the PI controller coefficients have been achieved as $K_p = 0.45$ and $K_i = 10$. Inner P current controller with Kp = 1.

For the traditional LQR control, $[q_1, q_2, q_3, q_4, r_1, r_2] = [1, 1, 1, 1000, 1, 1]$, and the optimal values for the GA-based LQR are achieved as $[q_1, q_2, q_3, q_4, r_1, r_2] = [2.849, 2.849, 0.884, 2447.735, 1.652, 1.652]$ and finally the best parameters were selected by the ICWOA $[q_1, q_2, q_3, q_4, r_1, r_2] = [2.511, 1.795, 1.326, 3416.59, 2.157, 2.314]$.

For analysis of the reliability of the proposed method and the state of art methods, digital simulation has been studied for a varied voltage from 0.8 s to 1 s with regards to load variation and between 1.4 s and 1.6 s with regard to air pressure variation (Habib et al., 2017) that is shown in Fig. 11. The first one due to the required load power variations. The second one is probably due to the oxygen or hydrogen pressure variations.

Fig. 12 shows the response of the controllers to the load current variation between 0 s and 2 s for the PEMFC. From Fig. 13, two different points are utilized for testifying the system: (i) a point with load current variation between 0 s and 1.4 s and (ii) a point with load current variation between 0.9 s and 1.8 s.

Simulation results show that the maximum value of the overshoot and the ripple belong to the classical PI controller. With regard to the validated results, it is clear that using the proposed converter can make a high reduction in the ripple and overshoot. It has been also observed that using the proposed optimization algorithms can easily make fast corrections than the classical PI controller. The properties of the proton exchange membrane are given in Table 3.

From Figs. 12 and 13, utilizing the proposed optimized method for driving the IBC converter to improve the voltage regulation efficiency are shown. The current ripples of the PEMFC are considerably minimized and consequently reduce the current limitations in the converter switches.

From Table 4, it is clear that the mean value of the maximum overshoot for two working points in the proposed ICWOA has the minimum value and the PI has the maximum value. From the results, it is observed that the overshoot value of the designed ICWOA method outperforms the original WOA method which shows the new algorithm's efficiency.

Table 4
ITAE test on the proposed controller and its comparison with the state-of-the-art methods.

	Point	Point 1	Point 2
Maximumovershoot (%)	PI (Wang and Ko, 2010)	95	70
	LQR (Habib and Khoucha, 2015)	69	65
	GA-LQR (Habib et al., 2017)	67	63
	WOA (Qazi et al., 2018)	67	65
	ICWOA	65	64
Ripple	PI (Wang and Ko, 2010)	0.15	0.14
	LQR (Habib and Khoucha, 2015)	0.11	0.05
	GA-LQR (Habib et al., 2017)	0.13	0.21
	WOA (Qazi et al., 2018)	0.14	0.01
	ICWOA	0.08	0.01

It can be also seen that the ripple value of the ICWOA for both working points 1 and 2 (8% and 1%) is the minimum value than the other methods, especially the original WOA method. Another result that can be concluded is that using the meta-heuristics improves the system efficiency both in the overshoot and the ripple toward the ordinary methods like PI controller and the traditional LQR.

The mean value of the ITAE for all the state of art methods is illustrated in Table 5. It is concluded that using the proposed ICWOA method by 4.12% has the minimum error than the other methods.

Finally, Table 6 illustrates the running time of each studied methods. By more considering the system, it is clear that using configuration based on the classic methods needs less time than the optimized methods (PI with 2 s and LQR by 3 s).

But, using the meta-heuristics in this configuration is a time-consuming process. However, the speed of the WCO based method is lower than the GA, using the proposed ICWA is less than GA which shows its improvement in the convergence speed. One other important thing is that because of the real-time applications, the controller parameters have been justified for once, the optimality of the method here is more important than the running time. As it is illustrated, the main purpose is to reduce system oscillations on the PEMFC to improve the lifetime of the system. In addition, using the current of both phases in the IBC, the stress value on power switches and the size of the designed coil has been minimized. In the following, the LQR controller is adopted for adjusting the voltage terminal. A new improved version of the whale optimization algorithm is also proposed for determining the optimal values of the LQR coefficients.

8. Conclusions

This study presents a new configuration for a proton exchange membrane fuel cell (PEMFC) based on a two-phase interleaved DC/DC boost converter. The main idea is to decrease the ripples on the fuel cell for enhancing the lifetime of the PEMFC. Furthermore, by shared use of the current in a fuel cell with both phases of the IBC, the value of the stress on power switches and the designed size for coils has been minimized. LQR optimal control is utilized for regulating the voltage terminal. In this paper, a new improved optimization algorithm based on whale optimization algorithm and chaotic theory has been proposed for optimal selection of the LQR coefficients based on the time-weighted absolute error (ITAE). The simulation results of the proposed optimized method are compared with four different control strategies and the final results showed a high improvement in the system from the point of decreasing the overshoot and current ripples.

Declaration of competing interest

The authors declare that they have no known competing financial interests or personal relationships that could have appeared to influence the work reported in this paper.

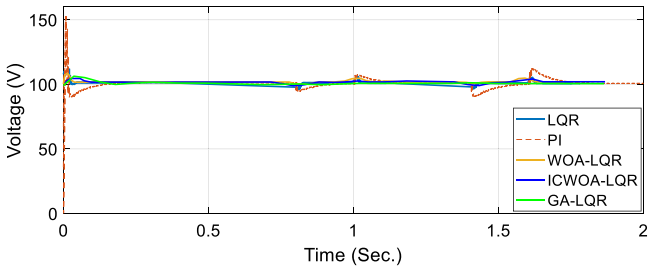

Fig. 12. The response of the controllers to load current variation (between 0 s and 2 s) for the PEMFC.

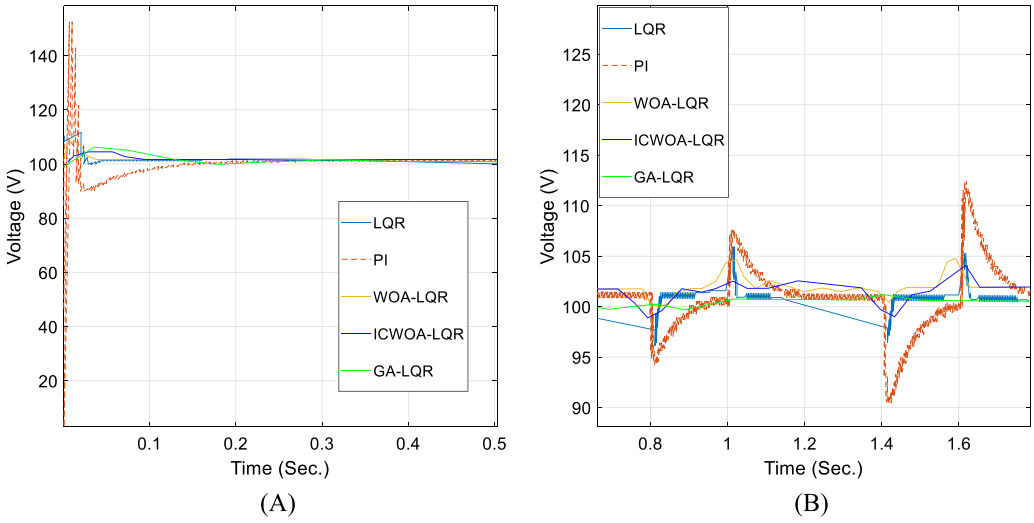

Fig. 13. Focused on the above figure to illustrate the amount of overshoot and ripple in point 1 (A) and point 2 (B).

Table 5
Total ITAE for the methods.

Method	PI (Wang and Ko, 2010)	LQR (Habib and Khoucha, 2015)	GA-LQR (Habib et al., 2017)	WOA (Qazi et al., 2018)	ICWOA
Value (%)	7.51	6.47	4.40	4.59	4.12

Table 6
Real-time validation of the system based on the system running time.

Method	Running time (s)
PI (Wang and Ko, 2010)	2
LQR (Habib and Khoucha, 2015)	3
GA-LQR (Habib et al., 2017)	15
WOA (Qazi et al., 2018)	17
ICWOA	13

CRediT authorship contribution statement

Yan Cao: Conceptualization, Data curation, Writing - original draft, Writing - review & editing. **Yiqing Li:** Conceptualization, Data curation, Writing - original draft, Writing - review & editing. **Geng Zhang:** Conceptualization, Data curation, Writing - original draft, Writing - review & editing. **Kittisak Jermsittiparsert:** Conceptualization, Data curation, Writing - original draft, Writing - review & editing. **Maryam Nasseri:** Conceptualization, Data curation, Writing - original draft, Writing - review & editing.

Acknowledgments

This paper is supported by Shaanxi Innovation Capability Support Plan, China (Grant: 2018TD-036), Shaanxi Key Research and Development Plan, China (Grant: 2018ZDXM-GY-077), Project of Joint Postgraduate Training Base of Xi'an Technological University, China, and Research Project of Graduate Education, China and Teaching Reform of Xi'an Technological University in 2017, China.

References

Aghajani, Gholamreza, Ghadimi, Noradin, 2018. Multi-objective energy management in a micro-grid. Energy Rep. 4, 218–225.

Ahmadi, S., Abdi, S., Kakavand, M., 2017. Maximum power point tracking of a proton exchange membrane fuel cell system using PSO-PID controller. Int. J. Hydrogen Energy 42, 20430–20443.

Ahmadi, P., Kjeang, E., 2015. Comparative life cycle assessment of hydrogen fuel cell passenger vehicles in different Canadian provinces. Int. J. Hydrog. Energy 40, 12905–12917.

Ajasa, A.A., Sebiotimo, A.-A.A., THE use of matlab in the solution of linear quadratic regulator (LQR) problems.

Akbary, Paria, et al., 2019. Extracting appropriate nodal marginal prices for all types of committed reserve. Comput. Econ. 53 (1), 1–26.

Al-Saffar, M.A., Ismail, E.H., 2015. A high voltage ratio and low stress DC–DC converter with reduced input current ripple for fuel cell source. Renew. Energy 82, 35–43.

Alizadeh, E., Barzegari, M., Momenifar, M., Ghadimi, M., Saadat, S., 2016. Investigation of contact pressure distribution over the active area of PEM fuel cell stack. Int. J. Hydrogen Energy 41, 3062–3071.

Bandaghiri, P.S., Moradi, N., Tehrani, S.S., 2016. Optimal tuning of PID controller parameters for speed control of DC motor based on world cup optimization algorithm. Parameters 1, 2.

Banerjee, S., Ghosh, A., Rana, N., 2017. An improved interleaved boost converter with PSO-based optimal type-III controller. IEEE J. Emerg. Sel. Top. Power Electron. 5, 323–337.

Bansal, J.C., 2019. Particle swarm optimization. In: Evolutionary and Swarm Intelligence Algorithms. ed: Springer, pp. 11–23.
Basit, M.A., Badar, R., 2018. Online adaptive neurofuzzy based energy management schemes for fuel-cell based hybrid power system. In: 2018 14th International Conference on Emerging Technologies (ICET). pp. 1–6.
Buswig, Y.M., Othman, A.-K., Julai, N., Yi, S.S., Utomo, W.M., Siang, A.J.L.M., 2018. Voltage tracking of a multi-input interleaved buck-boost DC-DC converter using artificial neural network control. J. Telecommun. Electron. Comput. Eng. (JTEC) 10, 29–32.
Dwari, S., Parsa, L., 2011. An efficient high-step-up interleaved DC–DC converter with a common active clamp. IEEE Trans. Power Electron. 26, 66–78.
Ebrahimian, Homayoun, et al., 2018. The price prediction for the energy market based on a new method. Econ. Res.-Ekonom. istraž. 31 (1), 313–337.
Ghadimi, Noradin, Firouz, Mansour Hosseini, 2015. Short-term management of hydro-power systems based on uncertainty model in electricity markets. J. Power Technol. 95 (4), 265–272.
Giral, R., Martinez-Salamero, L., Leyva, R., Maixe, J., 2000. Sliding-mode control of interleaved boost converters. IEEE Trans. Circuits Syst. I 47, 1330–1339.
Gollou, Abbas Rahimi, Ghadimi, Noradin, 2017. A new feature selection and hybrid forecast engine for day-ahead price forecasting of electricity markets. J. Intell. Fuzzy Systems 32 (6), 4031–4045.
Guida, V., Guilbert, D., Douine, B., 2019. Literature survey of interleaved DC-DC step-down converters for proton exchange membrane electrolyzer applications. Trans. Environ. Electr. Eng. 3, 33–43.
Guilbert, D., Guarisco, M., Gaillard, A., N'Diaye, A., Djerdir, A., 2015. FPGA based fault-tolerant control on an interleaved DC/DC boost converter for fuel cell electric vehicle applications. Int. J. Hydrog. Energy 40, 15815–15822.
Gules, R., Pfitscher, L.L., Franco, L.C., 2003. An interleaved boost DC-DC converter with large conversion ratio. In: 2003 IEEE International Symposium on Industrial Electronics (Cat. No. 03TH8692). pp. 411–416.
Habib, M., Khoucha, F., 2015. An improved LQR-based controller for PEMFC interleaved DC-DC converter. Balkan J. Electr. Comput. Eng. 3, 30–35.
Habib, M., Khoucha, F., Harrag, A., 2017. GA-based robust LQR controller for interleaved boost DC–DC converter improving fuel cell voltage regulation. Electr. Power Syst. Res. 152, 438–456.
Hameed, W.I., Sawadi, B.A., Fadhil, A.M., 2018. Voltage tracking control of DC-DC boost converter using fuzzy neural network. Int. J. Power Electron. Drive Syst. 9, 1657–1665.
Hamian, Melika, et al., 2018. A framework to expedite joint energy-reserve payment cost minimization using a custom-designed method based on Mixed Integer Genetic Algorithm. Eng. Appl. Artif. Intell. 72, 203–212.
Hegazy, O., Van Mierlo, J., Lataire, P., 2012. Analysis, modeling, and implementation of a multidevice interleaved DC/DC converter for fuel cell hybrid electric vehicles. IEEE Trans. Power Electron. 27, 4445–4458.
Hespanha, J.P., 2005. Lecture notes on lqr/lqg controller design. In: Knowledge Creation Diffusion Utilization.
Holland, J.H., 1992. Genetic algorithms. Sci. Am. 267, 66–73.
Huangfu, Y., Zhuo, S., Chen, F., Pang, S., Zhao, D., Gao, F., 2017. Robust voltage control of floating interleaved boost converter for fuel cell systems. IEEE Trans. Ind. Appl. 54, 665–674.
Jabbari, Z., Nassernejad, B., Fallah, N., Javanbakht, M., Afsham, N., 2019. Fabrication of novel binderless anode via electrophoretic deposition for HT-PEMFC. Surf. Eng. 1–8.
Jalili, Aref, Ghadimi, Noradin, 2016. Hybrid harmony search algorithm and fuzzy mechanism for solving congestion management problem in an electricity market. Complexity 21 (S1), 90–98.
Jin, K., Ruan, X., Yang, M., Xu, M., 2006. A novel hybrid fuel cell power system. In: 2006 37th IEEE Power Electronics Specialists Conference. pp. 1–7.
Khalilpour, M., Valipour, K., Shayeghi, H., Razmjooy, N., 2013. Designing a robust and adaptive PID controller for gas turbine connected to the generator. Res. J. Appl. Sci. Eng. Technol. 5, 1544–1551.
Khodaei, Hossein, et al., 2018. Fuzzy-based heat and power hub models for cost-emission operation of an industrial consumer using compromise programming. Appl. Therm. Eng. 137, 395–405.
Kolli, A., Gaillard, A., De Bernardinis, A., Bethoux, O., Hissel, D., Khatir, Z., 2015. A review on DC/DC converter architectures for power fuel cell applications. Energy Convers. Manage. 105, 716–730.
Kwakernaak, H., Sivan, R., 1972. Linear Optimal Control Systems, Vol. 1. Wiley-interscience New York.
Lee, H., Song, H., Kim, J., 2006. Effect of reverse voltage on proton exchange membrane fuel cell performance. In: 2006 International Forum on Strategic Technology. pp. 205–208.
Leng, Hua, et al., 2018. A new wind power prediction method based on ridgelet transforms, hybrid feature selection and closed-loop forecasting. Adv. Eng. Inf. 36, 20–30.
Liu, Yang, Wang, Wei, Ghadimi, Noradin, 2017. Electricity load forecasting by an improved forecast engine for building level consumers. Energy 139, 18–30.
Lü, X., Miao, X., Liu, W., Lü, J., 2018. Extension control strategy of a single converter for hybrid PEMFC/battery power source. Appl. Therm. Eng. 128, 887–897.
Ma, R., Wu, Y., Breaz, E., Huangfu, Y., Briois, P., Gao, F., 2018. High-order sliding mode control of DC-DC converter for PEM fuel cell applications. In: 2018 IEEE Industry Applications Society Annual Meeting (IAS). pp. 1–7.
Mafarja, M.M., Mirjalili, S., 2017. Hybrid Whale Optimization Algorithm with simulated annealing for feature selection. Neurocomputing 260, 302–312.
Mayo-Maldonado, J.C., Valdez-Resendiz, J.E., Sanchez, V.M., Rosas-Caro, J.C., Claudio-Sanchez, A., Puc, F.C., 2019. A novel PEMFC power conditioning system based on the interleaved high gain boost converter. Int. J. Hydrogen Energy 44, 12508–12514.
Mekhilef, S., Saidur, R., Safari, A., 2012. Comparative study of different fuel cell technologies. Renew. Sustain. Energy Rev. 16, 981–989.
Mirjalili, S., 2019. Genetic algorithm. In: Evolutionary Algorithms and Neural Networks. ed: Springer, pp. 43–55.
Mirjalili, S., Lewis, A., 2016. The whale optimization algorithm. Adv. Eng. Softw. 95, 51–67.
Mirzapour, Farzaneh, et al., 2019. A new prediction model of battery and wind-solar output in hybrid power system. J. Ambient Intell. Hum. Comput. 10 (1), 77–87.
Moallem, P., Razmjooy, N., 2012. Optimal threshold computing in automatic image thresholding using adaptive particle swarm optimization. J. Appl. Res. Technol. 10, 703–712.
Morsali, Roozbeh, et al., 2014. A new multiobjective procedure for solving nonconvex environmental/economic power dispatch. Complexity 20 (2), 47–62.
Morsali, Roozbeh, et al., 2015. Solving a novel multiobjective placement problem of recloser and distributed generation sources in simultaneous mode by improved harmony search algorithm. Complexity 21 (1), 328–339.
Mousavi, B.S., Soleymani, F., 2014. Semantic image classification by genetic algorithm using optimised fuzzy system based on Zernike moments. Signal Image Video Process. 8, 831–842.
Mousavi, B.S., Soleymani, F., Razmjooy, N., 2013. Color image segmentation using neuro-fuzzy system in a novel optimized color space. Neural Comput. Appl. 23, 1513–1520.
Murray, R., 2010. Optimization-Based Control: Control and Dynamical Systems. California Institute of Technology, Pasadena.
Mwinga, M., Groenewald, B., McPherson, M., 2018. A DC–DC converter for PEMFC stack power conditioning applications. J. Phys.: Conf. Ser. 012086.
Nazarathy, Y., Pulemotov, A., 2012. MATH4406 (Control Theory) Unit 6: The Linear Quadratic Regulator (LQR) and Model Predictive Control (MPC), ed: September.
Oliva, D., El Aziz, M.A., Hassanien, A.E., 2017. Parameter estimation of photovoltaic cells using an improved chaotic whale optimization algorithm. Appl. Energy 200, 141–154.
Qazi, S., Mustafa, M., Sultana, U., Mirjat, N., Soomro, S., Rasheed, N., 2018. Regulation of voltage and frequency in solid oxide fuel cell-based autonomous microgrids using the whales optimisation algorithm. Energies 11 (1318).
Razmjooy, N., Khalilpour, M., 2015. A new design for PID controller by considering the operating points changes in Hydro-Turbine Connected to the equivalent network by using Invasive Weed Optimization (IWO) Algorithm. Int. J. Inf. Secur. Syst. Manage. 4, 468–475.
Razmjooy, N., Khalilpour, M., Ramezani, M., 2016a. A new meta-Heuristic optimization algorithm inspired by FIFA world cup competitions: Theory and its application in PID designing for AVR system. J. Control Autom. Electr. Syst. 27, 419–440.
Razmjooy, N., Madadi, A., Alikhani, H.-R., Mohseni, M., 2014. Comparison of LQR and pole placement design controllers for controlling the inverted pendulum. J. World's Electr. Eng. Technol. 2322, 5114.
Razmjooy, N., Madadi, A., Ramezani, M., Robust control of power system stabilizer using world cup optimization algorithm.
Razmjooy, N., Ramezani, M., Training wavelet neural networks using hybrid particle swarm optimization and gravitational search algorithm for system identification.
Razmjooy, N., Ramezani, M., 2014. An improved quantum evolutionary algorithm based on invasive weed optimization. Indian J. Sci. Res. 4, 413–422.
Razmjooy, N., Ramezani, M., Ghadimi, N., 2017. Imperialist competitive algorithm-based optimization of neuro-fuzzy system parameters for automatic red-eye removal. Int. J. Fuzzy Syst. 19, 1144–1156.
Razmjooy, N., Ramezani, M., Namadchian, A., 2016b. A new lqr optimal control for a single-link flexible joint robot manipulator based on grey wolf optimizer. Majlesi J. Electr. Eng. 10, 53.
Razmjooy, N., Shahrezaee, M., Solving ordinary differential equations using world cup optimization algorithm.
Razmjooy, N., Sheykhahmad, F.R., Ghadimi, N., 2018. A hybrid neural network–world cup optimization algorithm for melanoma detection. Open Med. 13, 9–16.
Reddy, K.J., Sudhakar, N., 2018. High voltage gain interleaved boost converter with neural network based MPPT controller for fuel cell based electric vehicle applications. IEEE Access 6, 3899–3908.
Sabzali, A.J., Ismail, E.H., Behbehani, H.M., 2015. High voltage step-up integrated double Boost–Sepic DC–DC converter for fuel-cell and photovoltaic applications. Renew. Energy 82, 44–53.

Sanghavi, B., Tejaswini, C., Venkateshappa, V., 2019. DC/DC boost converter using DSP controller for fuel cell. In: Perspectives in Communication, Embedded-Systems and Signal-Processing-PiCES, Vol. 2. pp. 248–251.
Schymura, C., Kolossa, D., 2019. Learning dynamic stream weights for linear dynamical systems using natural evolution strategies. In: ICASSP 2019-2019 IEEE International Conference on Acoustics, Speech and Signal Processing (ICASSP). pp. 7893–7897.
Shahrezaee, M., 2017. Image segmentation based on world cup optimization algorithm. Majlesi J. Electr. Eng. 11.
Wang, H., Gaillard, A., Hissel, D., 2019. A review of DC/DC converter-based electrochemical impedance spectroscopy for fuel cell electric vehicles. Renew. Energy.
Wang, F.-C., Ko, C.-C., 2010. Multivariable robust PID control for a PEMFC system. Int. J. Hydrogen Energy 35, 10437–10445.
Yan, C., Chen, J., Liu, H., Lu, H., 2019. Model-based fault tolerant control for the thermal management of PEMFC systems. IEEE Trans. Ind. Electron..
Yang, D., Li, G., Cheng, G., 2007. On the efficiency of chaos optimization algorithms for global optimization. Chaos Solitons Fractals 34, 1366–1375.
Zhang, Y., Fu, C., Sumner, M., Wang, P., 2017. A wide input-voltage range quasi-Z-source boost dc–dc converter with high-voltage gain for fuel cell vehicles. IEEE Trans. Ind. Electron. 65, 5201–5212.
Zhang, H., Hui, Q., 2016. Parallel multiagent coordination optimization algorithm: Implementation, evaluation, and applications. IEEE Trans. Autom. Sci. Eng. 14, 984–995.